

# Can Transverse Mass Scaling Shed Light on the Event-Activity Dependence of $\Upsilon$ Mesons Production at LHC?

Iakov Aizenberg,<sup>1</sup> Zvi Citron,<sup>2</sup> and Alexander Milov<sup>1,\*</sup>

<sup>1</sup>*Department of Physics and Astrophysics, Weizmann Institute of Science, Rehovot, 761001, Israel*

<sup>2</sup>*Department of Physics, Ben Gurion University of the Negev, Beer Sheva, 8410501, Israel*

(Dated: January 11, 2023)

Measurements by the CMS experiment [1, 2] reveal a deficit of charged particle tracks in events with higher  $\Upsilon$ (nS) states. This observation is suggested to be a manifestation of the excited bottomonia suppression in  $pp$  interactions. Transverse mass ( $m_T$ ) scaling can be implied to check this assumption in an independent way. The scaling has been observed for a wide range of particle species in proton-proton collisions at various energies from the SPS to RHIC and the LHC. The observed scaling is known to be different for baryons and mesons, and this work presents a comprehensive study of the  $m_T$ -scaling of mesons at LHC energies with a focus on heavier mesons. The study demonstrates patterns in the scaling properties of mesons, which are related to the particle quark content. In particular, light species and ground-state quarkonia obey the same scaling, whereas open-flavor particles deviate from it because their spectra are significantly harder. The magnitude of deviation depends on the flavor of the heaviest quark in the meson. By extending the  $m_T$ -scaling assumption to the excited bottomonia states, it is observed that the measured cross sections of  $\Upsilon$ (2S) and  $\Upsilon$ (3S) are reduced by factors of 1.6 and 2.4 compared to the expectation from the scaling. This observation is consistent with recently observed differences between the event-activity dependence of different  $\Upsilon$ (nS) meson states.

Keywords: transverse-mass scaling, quarkonia, heavy flavor

## I. INTRODUCTION

Based on a statistical thermodynamical approach, it was suggested [3] that hadron production in proton-proton ( $pp$ ) collisions scales with the transverse mass of the produced particles. Transverse mass is defined as  $m_T = \sqrt{p_T^2 + m_0^2}$ , where  $p_T$  is the momentum of the hadron in the plane orthogonal to the collision axis, and  $m_0$  is its rest mass. This scaling was demonstrated experimentally in measurements at the ISR experiment [4, 5]. Although no longer thought to represent a fundamental hadronic temperature as originally proposed, it has since been used by many experiments and phenomenological studies to understand particle production in  $pp$  and nucleus-nucleus collisions from the SPS to RHIC and the LHC [6–8]. The original expression of  $m_T$ -scaling [3] used an exponential form, but it may also be derived based on Tsallis statistics [9] in which a power law provides a better description of particle spectra at higher collision energies ( $\sqrt{s}$ ). Various extensions of the transverse-mass scaling incorporate different assumptions and are capable of describing a broad variety of experimental data with impressive precision [10]. In this letter, an assumption of  $m_T$  scaling is used to provide a qualitative corollary to measurements of  $\Upsilon$  mesons made by the CMS experiment in  $pp$  collisions [1, 2]. CMS observed an intriguing correlation between the order of the  $\Upsilon$ (nS)-meson state and the multiplicity of charged hadrons measured in  $pp$  collisions and suggested that this may correspond to a suppression of the excited  $\Upsilon$ (nS) states. In this analysis, the  $m_T$ -scaling assumption is used to define a baseline for excited  $\Upsilon$  meson production from which suppression could be estimated.

The differential production cross-section can be approximated with the form

$$\frac{d^2\sigma}{dydm_T} \propto \left(1 + \frac{m_T}{nT}\right)^{-n} \quad (1)$$

which is derived from Tsallis statistics [10, 11]. In addition to  $m_T$ , the cross-section in the left-hand side of Eq. (1) is written as differential also in rapidity,  $y = \frac{1}{2} \ln [(E + p_z)/(E - p_z)]$ , where  $E$  is the energy of a particle and  $p_z$  is the momentum component in the direction of colliding protons. In principle,  $y$  factorizes from Eq. (1), but in practice, a weak dependence of the parameters in the right-hand side of Eq. (1) on  $y$  remains in the data [10]. Transverse mass scaling assumes that the exponent  $n$  and parameter  $T$  are universal for all particles for a given  $\sqrt{s}$ . It has been shown in many papers that mesons and baryons do not obey the same scaling (e.g., [8] and references therein). The analysis

---

\* alexander.milov@weizmann.ac.il

presented in this letter considers only mesons. The scaling behavior of heavy mesons is studied in comparison to light quark species and is used to understand the ratios between excited and ground quarkonia states measured in experiments.

## II. EXPERIMENTAL DATA

The experimental data used in this work is drawn from  $pp$  collisions at  $\sqrt{s} = 7, 8,$  and  $13$  TeV measured by the ALICE [12–24], ATLAS [25–32], CMS [33–43], and LHCb [44–55] experiments. The data are obtained from the HEP database and processed using the following procedure:

- Only measurements of mesons are considered.
- Where available, the prompt production component is used. For charmonia states, this excludes feed-down contributions from  $B$  mesons but includes the feed-down from decays of heavier charmonium states. These processes may contribute more than 30% of the measured charmonium cross section [34], and the analogous contribution to bottomonium states may be even larger [56].
- For measurements which are corrected using multiple meson polarization assumptions, the results corresponding to the zero polarization assumption are selected.
- Measurements reported within a detector’s fiducial acceptance are corrected to the total cross-sections using the zero polarization assumption.
- Since particle ratios for quarkonia states considered in this letter are typically measured in dilepton decays channels, the particle ratios also include branching ratios.
- Cross-sections measured to rapidity larger than 3 but reported differentially in rapidity are selected with  $|y| < 3$  for better consistency with the results measured at mid-rapidity.

The collected data contains 88 independent measurements of particle species and 18 measurements of the particle ratios, spanning transverse momentum from 0 to 150 GeV and absolute rapidity from 0 to 4.5. Measurements that contain less than 5 data points or span less than several GeV in transverse momentum are not used in the analysis. Where multiple measurements of the same particle are reported by the same experiment at the same energy, the measurements typically rely on different statistical samples and therefore are considered to be independent. They are combined using a constant scaling factor applied to one of the measurements. This factor is calculated to account for small differences in the properties of the different measurements, for example, the rapidity coverage. The magnitude of the factor is close or equal to unity. Measurements of isospin-partner particles made by the same experiment and measurements of the same particles performed by different experiments are not combined.

Altogether, this analysis uses 72 combined data samples of 18 particle species and their isospin partners with 1509 experimental data points and 15 measurements of particle ratios with 327 data points.

## III. FITS

Each data sample is fitted to the functional form given by Eq. (1). Point-by-point uncorrelated uncertainties are used in the fits. Point-by-point fully correlated uncertainties (scaling factors) are not considered because the spectra of different particles are re-normalized in the analysis. Other point-by-point correlated uncertainties are shown in the relevant figures but are not input into the fits.

In addition to the general data handling discussed above, several data exclusions are made in the fitting procedure. Measurements of  $\pi^0$  and  $\pi^\pm$  with  $p_T < 2$  GeV are excluded based on the considerations discussed in Refs. [8, 16]. Low momentum,  $p_T < 5$  GeV,  $\Upsilon$  meson measurements are also excluded from the fitting because in the low momentum region, there is a large contribution from  $\chi_b(mP) \rightarrow \Upsilon(nS)\gamma$  decays with  $m \geq n$ . A correction for feed-down decays from heavier mesons ( $\chi_c, \chi_b$ ) is not applied because it cannot be reliably determined from existing data, although it is expected to be similar in magnitude for all  $\Upsilon(nS)$  states [57].

Since the fit parameters  $T$  and  $n$  are strongly correlated with each other, unconstrained fits produce results that are difficult to interpret in a coherent way. Therefore, the parameter  $T$  is fixed to 254 MeV for all analyzed particles. This value is obtained from a simultaneous fit to several selected data sets at  $\sqrt{s} = 7$  GeV and is close to the value of the same parameter used in [8]. The exponent,  $n$ , obtained from the fits is plotted versus the particle rest mass in Figure 1.

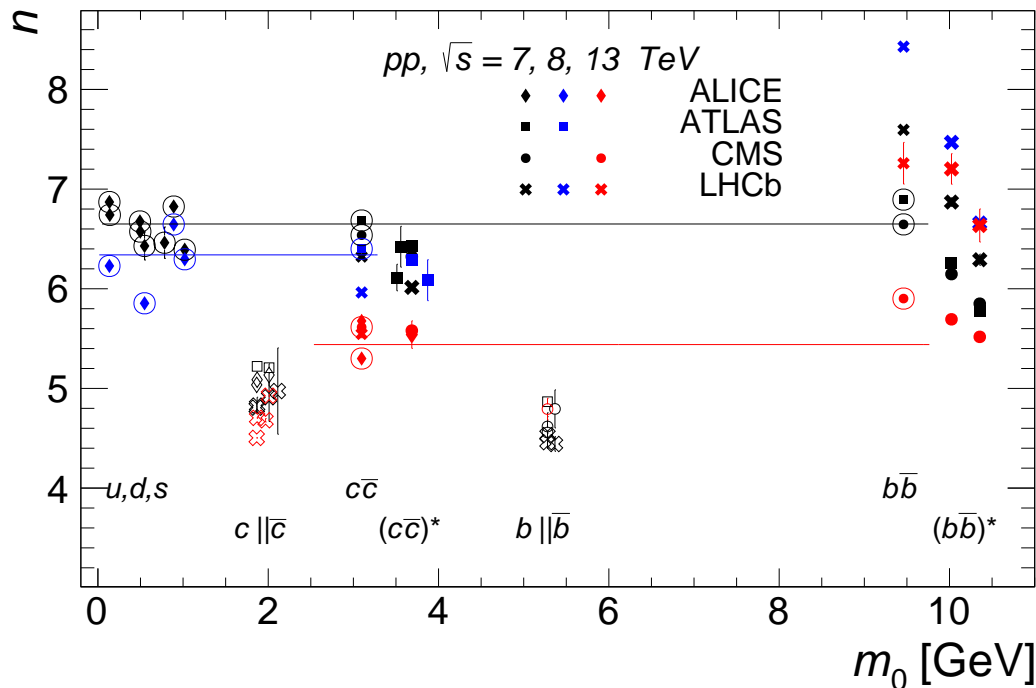


FIG. 1. Color online. The mass dependence of the  $m_T$ -spectra exponent  $n$  for different measured species. Symbol shapes denote experiments, open symbols denote open heavy flavor particles, and larger symbols denote excited quarkonia states. Error bars are uncertainties of the fits. Encircled points indicate the results which are used for common fits of the  $u,d,s$  and ground-state  $q\bar{q}$  mesons. The results of these fits are shown by horizontal lines. Different colors represent different collision energies.

There are several patterns visible in the figure. Particles produced in collisions with higher  $\sqrt{s}$  have harder spectra which corresponds to lower values of  $n$ , given a fixed  $T$ . LHCb results for  $\mathcal{T}$  are higher at each collision energy because they are measured at higher rapidity  $2 < |y| < 3$ . Comparing results at the same energy shows that  $n$  increases with rapidity, reflecting the fact that particle spectra become softer at high rapidity [10]. Several other measurements of light mesons that are made at high rapidity also show higher  $n$ , they are not plotted in Figure 1 for plot clarity.

The magnitude of  $n$  obtained from the fits shows a strong dependence on the quark content of the particle. Open heavy flavor mesons ( $q||\bar{q}$ ) demonstrate much harder spectra compared to other species. This holds for all energies, and the effect is stronger for open bottom ( $b||\bar{b}$ ) than for open charm ( $c||\bar{c}$ ).

As has been observed in [10], at LHC and lower energies, light particle species ( $u,d,s$ ) and quarkonia states follow  $m_T$ -scaling, i.e., their spectral distributions can be fitted to Eq. (1), or to the Tsallis form [9], with the same parameters  $T$  and  $n$ . In a large number of publications, the same statement is derived for narrower selections of mesons, e.g., in [7, 11, 16].

Figure 1 shows that the values of  $n$  for  $u,d,s$  and ground-state heavy quarkonia ( $q\bar{q}$ ) mesons are similar. However, excited quarkonia states ( $(q\bar{q})^*$ ) have lower values of  $n$  than the ground state as seen by the ordering  $n(\mathcal{T}(1S)) > n(\mathcal{T}(2S)) > n(\mathcal{T}(3S))$ . A similar ordering of  $n$  for charmonia states,  $n(J/\Psi) > n(\Psi(2S))$ , may be present, although the effect is smaller than for bottomonia.

Based on these observations, the values of  $n$  for  $u,d,s$  and ground-state  $q\bar{q}$  mesons measured at midrapidity are fit. The selected data sets are indicated with circles around their markers in Figure 1. There are 12, 5, and 3 data samples at  $\sqrt{s} = 7, 8, \text{ and } 13$  TeV, respectively. The  $\sqrt{s} = 7$  TeV values are fit to a linear function which becomes a constant for a chosen value of parameter  $T$ . Due to the low number of selected data sets at higher energies, the 8 and 13 TeV data are fit to a constant. The values of  $n(\sqrt{s} = 7, 8, 13[\text{TeV}]) = (6.65, 6.34, 5.44)$ , and are used in the analysis described below. These values are shown in Figure 1 by horizontal lines. The quality of the fits and statistical uncertainties associated with the parameters are investigated in detail in a number of similar studies (e.g. [10, 58]). In this analysis, the robustness of the common fits are checked by changing  $T$  by  $\pm 50$  MeV, which shifts the points by approximately a unit but does not change the discussion or conclusions below.

Figure 2 shows the various measurements from all three collision energies, divided by the expectation from  $m_T$ -scaling in which  $n$  at each collision energy is fixed to the values mentioned above. The points which are used in the common fit are shown in gray, other points are shown in colors. Overall, points shown in gray demonstrate reasonable

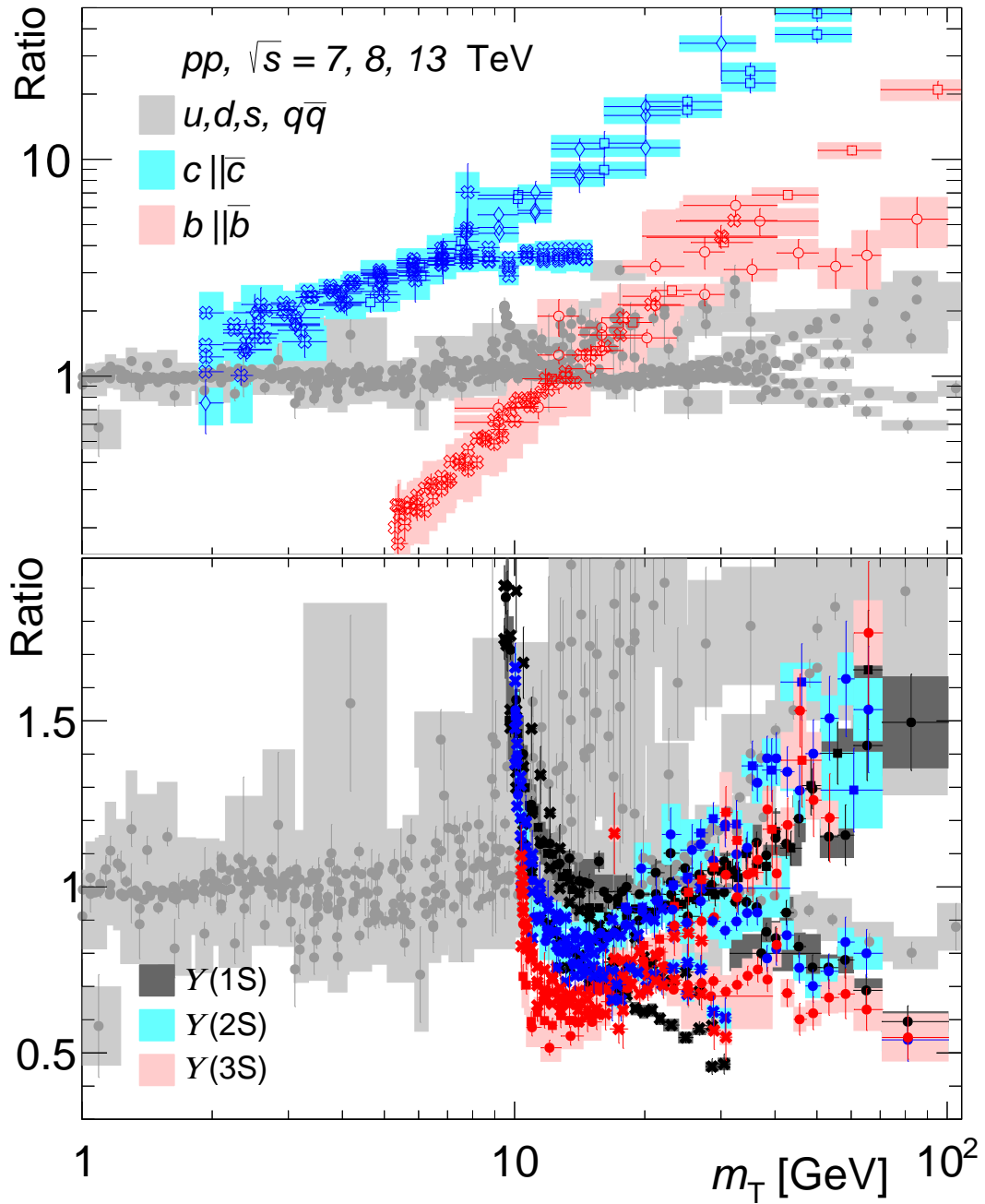


FIG. 2. Measurements used in the common fit are shown in gray. Symbols follow the notation of Figure 1. Individual curves of  $q||\bar{q}$  are scaled with arbitrary factors for visibility.

agreement with unity, although at high- $p_T$   $q\bar{q}$  spectra tend to rise deviating by up to a factor of 2, somewhat similar to what can be seen in Ref. [10]. Increasing  $n(\sqrt{s})$  can partially solve this problem, however, further optimizing the fit would be difficult without knowing the prompt components in the cross sections of heavier species. Taking this into account, and also given the ranges that the measurements cover in particle mass and  $p_T$ , the agreement to a common fit shown in the plot can be considered sufficient for the purposes of this analysis.

The upper panel of Figure 2 compares results measured for  $c||\bar{c}$  and  $b||\bar{b}$  with the results of the common fit. Individual  $q||\bar{q}$  measurements are vertically scaled with arbitrarily-chosen factors in the range 0.5–5 for the clarity of the plot. Differences in the slopes are expressions of the observation that  $b||\bar{b}$  has harder spectra, compared to  $c||\bar{c}$  and other particles, as seen in Figure 1.

A comparison of the measured  $b\bar{b}$  and  $(b\bar{b})^*$  states to the common fit is shown in the lower panel of Figure 2. This

figure shows all data, including measurements at forward rapidity and data points at  $p_T < 5$  GeV which are excluded from the fits. The splitting of  $\Upsilon(nS)$  points at high- $m_T$  is due to the  $\sqrt{s} = 13$  TeV measurements, whose  $n$  is not accurately reflected in the common fit due to a lack of experimental data as seen in Figure 1. A significant rise for all  $\Upsilon(nS)$  states at low  $p_T$ , i.e.,  $m_T$  only slightly above the  $\Upsilon$  mass, is clearly visible. The contribution of  $\chi_b(1P) \rightarrow \Upsilon(1S)$  has been estimated using PYTHIA8 [59] simulations and found to be qualitatively consistent with the large excess at  $m_T$  close to the  $\Upsilon(1S)$  mass seen in the Figure. Higher  $\chi_b$  states have not been simulated, but the similarity of the excess for  $\Upsilon(2S)$  and  $\Upsilon(3S)$  in the ratio at  $m_T$  close to the  $\Upsilon$  mass suggests that a significant contribution also of these likely comes from  $\chi_b$  decays and the non-prompt fraction of the different  $\Upsilon(nS)$  states is similar as expected [56, 57]. To check the effects of the non-prompt fraction varying between different  $\Upsilon(nS)$  states, the PYTHIA8 simulation for the  $\chi_b(1P) \rightarrow \Upsilon(nS)$  processes has been modeled with the same rate as the non-prompt yield of  $\Upsilon(1S)$ . Then the non-prompt yields into  $\Upsilon(1S)$  were increased by an additional 20%, i.e., nearly doubled. This is found not to affect the conclusions.

Since the meson ratios at high  $p_T$  are constant [30, 32, 34, 39, 40, 56],  $(b\bar{b})^*$  results shown in the figure are normalized to  $b\bar{b}$  at high- $p_T$  by scaling factors. All  $\Upsilon(2S)$  results are scaled by 0.9, and all  $\Upsilon(3S)$  results by 0.7. The lower panel of Figure 2 shows that, apart from the rise at low  $p_T$ ,  $\Upsilon(1S)$  follows the trend of particles included in the common fit. On the other hand, compared to  $b\bar{b}$  there is a clear deficit of  $(b\bar{b})^*$  states at low and intermediate  $p_T$ .

#### IV. DISCUSSION

The  $m_T$ -scaling phenomenon observed at lower  $\sqrt{s}$  and at LHC energies for  $u, d, s$  mesons approximately holds for heavier  $q\bar{q}$  particles in their ground state. Analysis of the LHC data shows that mesons obey or deviate from the scaling depending on the heaviest quark contained in the particle and whether quarks forming the meson are bound in the ground or excited state. Particles with an open charm or bottom have significantly harder spectra than all other particles, and  $b|\bar{b}$  mesons have a harder spectra than  $c|\bar{c}$  mesons.

Employing  $m_T$ -scaling to compare particle spectra distributions is a commonly-used technique, as it reproduces well the momentum dependence of a variety of experimentally measured particles [16]. In this letter,  $m_T$ -scaling is used to study the ratios of  $(q\bar{q})^*/q\bar{q}$  as is shown in the upper panel of Figure 3.

Since the particle ratios are known to only weakly depend on rapidity and  $\sqrt{s}$ , all available LHC data is shown in the same plot. The  $p_T$  dependence of the ratios is not trivial and is challenging for models to reproduce [57]. In this letter, the data is compared to expectations based on  $m_T$ -scaling, which are shown with solid lines for the three collision energies. The  $m_T$  expectations are normalized to data at  $p_T > 50$  GeV, and the uncertainties resulting from the normalization are shown with thin lines. There are clear differences between the expectation and the data for  $(b\bar{b})^*$  species and a significantly better consistency for  $(c\bar{c})^*$ .

To quantify the discrepancies, the lower panel shows the particles' 'missing fraction' constructed from the ratios. It is the measured value subtracted from the expected value and normalized to the measured, this normalization cancels the ground state production rate, and thus the quantity represents the 'missing' excited state production equal to  $(q\bar{q})_{\text{expected}}^*/(q\bar{q})_{\text{measured}}^* - 1$ . The normalization uncertainty is added to the systematic uncertainty drawn at each point. The curves show that assuming the  $m_T$ -scaling scenario and  $\Upsilon(1S)$ -meson cross-section, at low  $p_T$  the  $\Upsilon(2S)$  production expectation is approximately twice as high as the measurement and  $\Upsilon(3S)$  is roughly three times higher. Estimation for  $\Psi(2S)$  at low  $p_T$  is above zero, suggesting that the  $(c\bar{c})^*$  may also be affected, although to a much lesser extent than the  $\Upsilon$  case. With the existing data and understanding of the prompt fraction in  $J/\Psi$ , a conclusion about  $(c\bar{c})^*$  cannot be drawn with a large degree of certainty. At higher  $p_T$ ,  $\Upsilon(2S)$  and  $\Upsilon(3S)$  points are significantly above zero to at least 30 GeV.

The observations reported here may share a common origin with the results reported in [2]. The CMS collaboration measured the production of  $\Upsilon(nS)$  mesons at  $\sqrt{s} = 7$  GeV as a function of the charged particle multiplicity in the underlying event. CMS observed that events containing  $\Upsilon(1S)$  meson measure about two more tracks than events with  $\Upsilon(3S)$  and one more track than events with  $\Upsilon(2S)$ . The CMS collaboration noted that suppression of the  $(b\bar{b})^*$  states at high multiplicity in  $pp$  collisions can produce the measured effect. This assumption is qualitatively consistent with the discrepancy between the  $(b\bar{b})^*$  production rates measured by the LHC experiments and their expectations from the  $m_T$ -scaling assumption that is plotted in Figure 3.

If fewer tracks in collisions with  $(b\bar{b})^*$  as observed by CMS, and reduced production of higher  $\Upsilon(nS)$  mesons shown in Figure 3 are two manifestations of the same physics process, it would mean that the measured cross-sections of  $\Upsilon(2S)$  and  $\Upsilon(3S)$  mesons are 'suppressed' by factors of 1.6 and 2.4 compared to the expectation from the production rates of  $\Upsilon(1S)$  scaled by the missing fraction shown in the lower panel of Figure 3. A 5% uncertainty on these estimates is associated with the normalization uncertainties, and other effects, which are expressed as deviations from the common fit as discussed above, may have a comparable impact on the values. Nevertheless, they are too small to explain the gap between the  $m_T$ -scaling expected and measured ratios shown in the upper panel of Figure 3. The

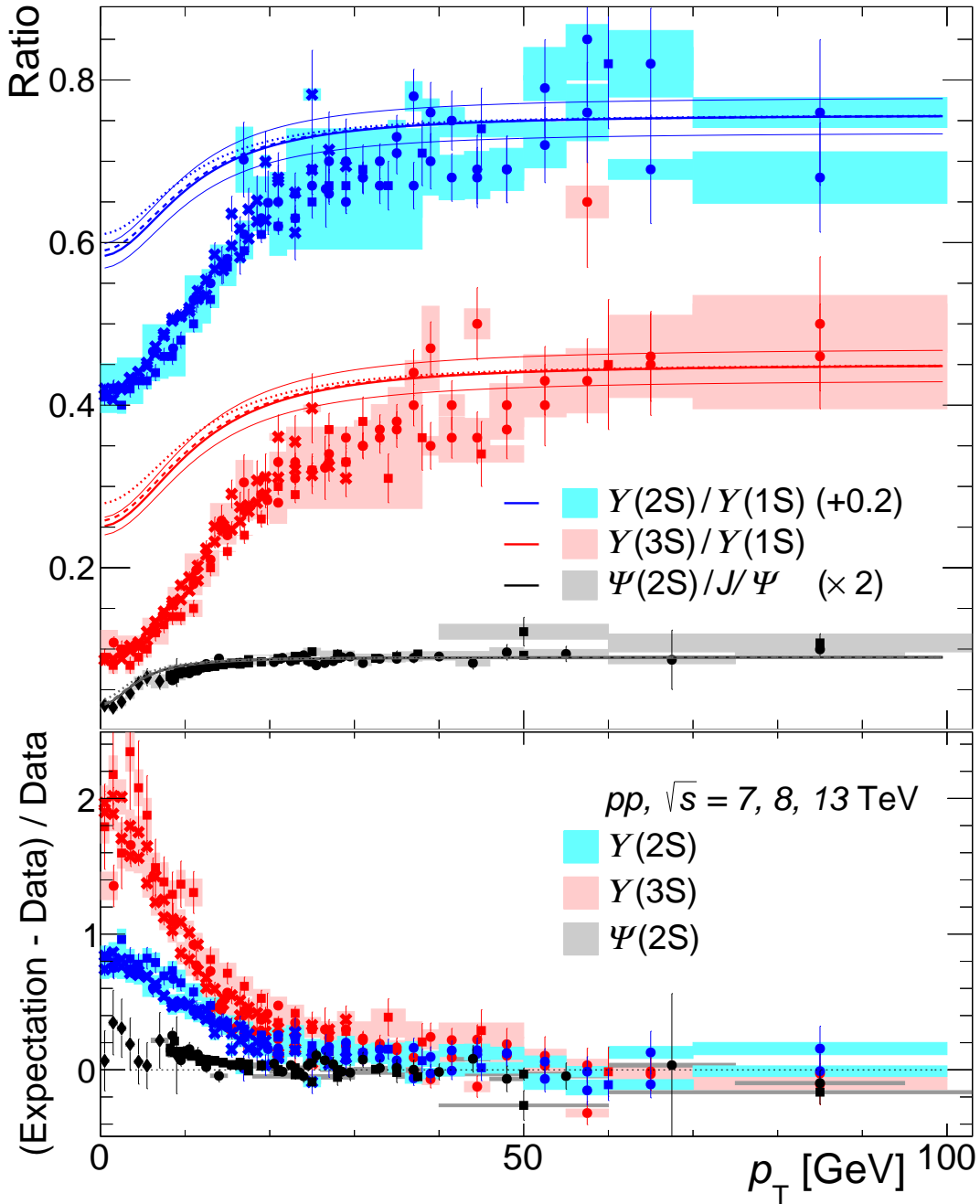


FIG. 3. Upper panel: Measured  $(q\bar{q})^*/q\bar{q}$  ratios are shown with markers.  $\Psi(2S)$  data is scaled, and  $Y(2S)$  data is shifted for plot clarity. Lines are expectations from the  $m_T$ -scaling prediction, normalized to the data in the region of  $p_T > 50$  GeV. The dashed (dotted) lines correspond  $\sqrt{s} = 8$  (13) TeV, and finer lines indicate the normalization uncertainty. Lower panel: The difference of the expected value based on  $m_T$ -scaling to the measurement divided by the measurement.

mechanism that suppresses the rates of  $(b\bar{b})^*$  may also affect production rates of other  $(q\bar{q})^*$  states, for example,  $\Psi(2S)$  shown in Figure 3, however, in this particular case the effect is visibly weaker. Any conclusion about modification of the production rate of the  $Y(1S)$ -meson itself, lies outside of the framework of this analysis, because it breaks the  $m_T$ -scaling assumption. Existing theoretical cross-section calculations [57, 60–63] show that the calculations generally better agree with the data for  $Y(1S)$ , compared to higher  $Y(nS)$ , but these calculations are not available in the low- $p_T$  region, where the discrepancy is the largest. Recently the comover interaction model successfully reproduced [64] event multiplicity dependence of the  $Y(nS)$  ratios measured by CMS. Theoretical interpretations of the effect that would simultaneously reproduce the suppression of excited  $Y(nS)$  states and reduction of tracks in the collisions are

needed.

## V. SUMMARY

A systematic analysis of transverse-momentum distributions of mesons produced in  $pp$  collisions at LHC energies suggests that the spectra of light mesons and ground state quarkonia particles have the same spectral shape, given by Eq. (1) with universal parameters  $T$  and  $n$  for a given collision energy. Open-heavy-flavor mesons with  $c$ -quark in them have significantly harder spectra, and open-flavor  $b$ -mesons even harder. Production rates of excited bottomonia states with respect to ground state are significantly suppressed at  $p_T$  approaching zero, with more suppression measured for the higher excited state. The effect diminishes with increasing  $p_T$  but remains significant at least up to 30 GeV. Production rates of  $\Upsilon(2S)$  and  $\Upsilon(3S)$  states are fewer by factors 1.6 and 2.4, respectively, than they would be anticipated from the  $m_T$ -scaling assumption. This suppression of higher  $\Upsilon(nS)$  qualitatively agrees with the effect observed in [1, 2] and may be a manifestation of the same physics phenomenon. Production rate of  $\Psi(2S)$  is generally consistent with the expectation from  $J/\Psi$ , although a smaller-magnitude suppression cannot be excluded. Current theoretical calculations can be advanced by relating the cross-section measurements to the event multiplicity.

## ACKNOWLEDGMENTS

Research of Z.C. is supported by the Israel Science Foundation (grant 1946/18). Research of I.A. and A.M. is supported by Israel Academy of Science and Humanity and the MINERVA Stiftung with the funds from the BMBF of the Federal Republic of Germany.

- 
- [1] S. Chatrchyan et al. (CMS), Event Activity Dependence of  $\Upsilon(nS)$  Production in  $\sqrt{s_{NN}} = 5.02$  TeV  $p$ +Pb and  $\sqrt{s} = 2.76$  TeV  $pp$  Collisions, JHEP **04**, 103, arXiv:1312.6300.
  - [2] A. M. Sirunyan et al. (CMS), Investigation into the event-activity dependence of  $\Upsilon(nS)$  relative production in  $pp$  collisions at  $\sqrt{s} = 7$  TeV, JHEP **11**, 001, arXiv:2007.04277.
  - [3] R. Hagedorn, Statistical thermodynamics of strong interactions at high energies, Nuovo Cimento, Suppl. **3**, 147 (1965).
  - [4] B. Alper et al., Large angle inclusive production of charged pions at the cern isr with transverse momenta less than 1.0 GeV/c, Phys. Lett. B **47**, 75 (1973).
  - [5] B. Alper, H. Boggild, P. Booth, F. Bulos, L. Carroll, G. Von Dardel, G. Damgaard, B. Duff, F. Heymann, J. Jackson, G. Jarlskog, L. Jonsson, A. Klovning, L. Leistam, E. Lillethun, G. Lynch, S. Olgaard-Nielsen, M. Prentice, D. Quarrie, and J. Weiss, Large-angle inclusive production of charged pions at the CERN ISR with transverse moment less than 1.0 GeV/c, Phys. Lett. B **47**, 75 (1973).
  - [6] E. L. Bratkovskaya, W. Cassing, and U. Mosel, Meson  $m_T$ - scaling in heavy ion collisions at SIS energies, Phys. Lett. B **424**, 244 (1998), arXiv:nucl-th/9712046.
  - [7] B. I. Abelev et al. (STAR), Strange particle production in  $pp$  collisions at  $\sqrt{s} = 200$ -GeV, Phys. Rev. C **75**, 064901 (2007), arXiv:nucl-ex/0607033.
  - [8] L. Altenkämper, F. Bock, C. Loizides, and N. Schmidt, Applicability of transverse mass scaling in hadronic collisions at energies available at the CERN Large Hadron Collider, Phys. Rev. C **96**, 064907 (2017), arXiv:1710.01933.
  - [9] C. Tsallis, Possible Generalization of Boltzmann-Gibbs Statistics, J. Statist. Phys. **52**, 479 (1988).
  - [10] S. Grigoryan, Using the Tsallis distribution for hadron spectra in  $pp$  collisions: Pions and quarkonia at  $\sqrt{s} = 5$ –13000 GeV, Phys. Rev. D **95**, 056021 (2017), arXiv:1702.04110.
  - [11] A. Adare et al. (PHENIX), Measurement of neutral mesons in  $pp$  collisions at  $\sqrt{s} = 200$  GeV and scaling properties of hadron production, Phys. Rev. D **83**, 052004 (2011), arXiv:1005.3674.
  - [12] B. Abelev et al. (ALICE), Neutral pion and  $\eta$  meson production in proton-proton collisions at  $\sqrt{s} = 0.9$  TeV and  $\sqrt{s} = 7$  TeV, Phys. Lett. B **717**, 162 (2012), arXiv:1205.5724.
  - [13] J. Adam et al. (ALICE), Multiplicity dependence of charged pion, kaon, and (anti)proton production at large transverse momentum in  $p$ +Pb collisions at  $\sqrt{s_{NN}} = 5.02$  TeV, Phys. Lett. B **760**, 720 (2016), arXiv:1601.03658.
  - [14] J. Adam et al. (ALICE), Measurement of pion, kaon and proton production in  $pp$  collisions at  $\sqrt{s} = 7$  TeV, Eur. Phys. J. C **75**, 226 (2015), arXiv:1504.00024.
  - [15] S. Acharya et al. (ALICE), Production of  $\omega$  mesons in  $pp$  collisions at  $\sqrt{s} = 7$  TeV, Eur. Phys. J. C **80**, 1130 (2020), arXiv:2007.02208.
  - [16] S. Acharya et al. (ALICE), Production of light-flavor hadrons in  $pp$  collisions at  $\sqrt{s} = 7$  and  $\sqrt{s} = 13$  TeV, Eur. Phys. J. C **81**, 256 (2021), arXiv:2005.11120.
  - [17] S. Acharya et al. (ALICE),  $K^*(892)^0$  and  $\phi(1020)$  production at midrapidity in  $pp$  collisions at  $\sqrt{s} = 8$  TeV, Phys. Rev. C **102**, 024912 (2020), arXiv:1910.14410.

- [18] S. Acharya et al. (ALICE), Measurement of  $D$ -meson production at mid-rapidity in  $pp$  collisions at  $\sqrt{s} = 7$  TeV, Eur. Phys. J. C **77**, 550 (2017), arXiv:1702.00766.
- [19] B. B. Abelev et al. (ALICE), Measurement of quarkonium production at forward rapidity in  $pp$  collisions at  $\sqrt{s} = 7$  TeV, Eur. Phys. J. C **74**, 2974 (2014), arXiv:1403.3648.
- [20] S. Acharya et al. (ALICE),  $\pi^0$  and  $\eta$  meson production in  $pp$  collisions at  $\sqrt{s} = 8$  TeV, Eur. Phys. J. C **78**, 263 (2018), arXiv:1708.08745.
- [21] J. Adam et al. (ALICE), Inclusive quarkonium production at forward rapidity in  $pp$  collisions at  $\sqrt{s} = 8$  TeV, Eur. Phys. J. C **76**, 184 (2016), arXiv:1509.08258.
- [22] S. Acharya et al. (ALICE), Inclusive  $J/\Psi$  production at midrapidity in  $pp$  collisions at  $\sqrt{s} = 13$  TeV, Eur. Phys. J. C **81**, 1121 (2021), arXiv:2108.01906.
- [23] S. Acharya et al. (ALICE), Energy dependence of forward-rapidity  $J/\Psi$  and  $\Psi(2S)$  production in  $pp$  collisions at the LHC, Eur. Phys. J. C **77**, 392 (2017), arXiv:1702.00557.
- [24] S. Acharya et al. (ALICE), Energy dependence of  $\phi$  meson production at forward rapidity in  $pp$  collisions at the LHC, Eur. Phys. J. C **81**, 772 (2021), arXiv:2105.00713.
- [25] G. Aad et al. (ATLAS), Measurement of  $D^{*\pm}$ ,  $D^\pm$  and  $D_s^\pm$  meson production cross sections in  $pp$  collisions at  $\sqrt{s} = 7$  TeV with the ATLAS detector, Nucl. Phys. B **907**, 717 (2016), arXiv:1512.02913.
- [26] G. Aad et al. (ATLAS), Measurement of the differential cross-sections of inclusive, prompt and non-prompt  $J/\Psi$  production in  $pp$  collisions at  $\sqrt{s} = 7$  TeV, Nucl. Phys. B **850**, 387 (2011), arXiv:1104.3038.
- [27] G. Aad et al. (ATLAS), Measurement of  $\chi_{c1}$  and  $\chi_{c2}$  production with  $\sqrt{s} = 7$  TeV  $pp$  collisions at ATLAS, JHEP **07**, 154, arXiv:1404.7035.
- [28] G. Aad et al. (ATLAS), Measurement of the differential cross-sections of prompt and non-prompt production of  $J/\Psi$  and  $\Psi(2S)$  in  $pp$  collisions at  $\sqrt{s} = 7$  and 8 TeV with the ATLAS detector, Eur. Phys. J. C **76**, 283 (2016), arXiv:1512.03657.
- [29] G. Aad et al. (ATLAS), Measurement of the differential cross-section of  $B^+$  meson production in  $pp$  collisions at  $\sqrt{s} = 7$  TeV at ATLAS, JHEP **10**, 042, arXiv:1307.0126.
- [30] G. Aad et al. (ATLAS), Measurement of  $\Upsilon$  production in 7 TeV  $pp$  collisions at ATLAS, Phys. Rev. D **87**, 052004 (2013), arXiv:1211.7255.
- [31] G. Aad et al. (ATLAS),  $K$ -short and  $\Lambda$  production in  $pp$  interactions at  $\sqrt{s} = 0.9$  and 7 TeV measured with the ATLAS detector at the LHC, Phys. Rev. D **85**, 012001 (2012), arXiv:1111.1297.
- [32] M. Aaboud et al. (ATLAS), Measurements of  $\Psi(2S)$  and  $X(3872) \rightarrow J/\Psi\pi^+\pi^-$  production in  $pp$  collisions at  $\sqrt{s} = 8$  TeV with the ATLAS detector, JHEP **01**, 117, arXiv:1610.09303.
- [33] V. Khachatryan et al. (CMS), Prompt and Non-Prompt  $J/\Psi$  Production in  $pp$  Collisions at  $\sqrt{s} = 7$  TeV, Eur. Phys. J. C **71**, 1575 (2011), arXiv:1011.4193.
- [34] V. Khachatryan et al. (CMS), Measurement of  $J/\Psi$  and  $\Psi(2S)$  Prompt Double-Differential Cross Sections in  $pp$  Collisions at  $\sqrt{s} = 7$  TeV, Phys. Rev. Lett. **114**, 191802 (2015), arXiv:1502.04155.
- [35] S. Chatrchyan et al. (CMS), Measurement of the  $B^0$  production cross section in  $pp$  Collisions at  $\sqrt{s} = 7$  TeV, Phys. Rev. Lett. **106**, 252001 (2011), arXiv:1104.2892.
- [36] V. Khachatryan et al. (CMS), Measurement of the  $B^+$  Production Cross Section in  $pp$  Collisions at  $\sqrt{s} = 7$  TeV, Phys. Rev. Lett. **106**, 112001 (2011), arXiv:1101.0131.
- [37] S. Chatrchyan et al. (CMS), Measurement of the  $B_s^0$  Production Cross Section with  $B_s^0 \rightarrow J/\Psi\phi$  Decays in  $pp$  Collisions at  $\sqrt{s} = 7$  TeV, Phys. Rev. D **84**, 052008 (2011), arXiv:1106.4048.
- [38] S. Chatrchyan et al. (CMS), Measurement of the  $\Upsilon(1S)$ ,  $\Upsilon(2S)$ , and  $\Upsilon(3S)$  Cross Sections in  $pp$  Collisions at  $\sqrt{s} = 7$  TeV, Phys. Lett. B **727**, 101 (2013), arXiv:1303.5900.
- [39] V. Khachatryan et al. (CMS), Measurements of the  $\Upsilon(1S)$ ,  $\Upsilon(2S)$ , and  $\Upsilon(3S)$  differential cross sections in  $pp$  collisions at  $\sqrt{s} = 7$  TeV, Phys. Lett. B **749**, 14 (2015), arXiv:1501.07750.
- [40] S. Chatrchyan et al. (CMS),  $J/\Psi$  and  $\Psi(2S)$  production in  $pp$  collisions at  $\sqrt{s} = 7$  TeV, JHEP **02**, 011, arXiv:1111.1557.
- [41] A. M. Sirunyan et al. (CMS), Measurement of charged pion, kaon, and proton production in  $pp$  collisions at  $\sqrt{s} = 13$  TeV, Phys. Rev. D **96**, 112003 (2017), arXiv:1706.10194.
- [42] A. M. Sirunyan et al. (CMS), Measurement of quarkonium production cross sections in  $pp$  collisions at  $\sqrt{s} = 13$  TeV, Phys. Lett. B **780**, 251 (2018), arXiv:1710.11002.
- [43] V. Khachatryan et al. (CMS), Measurement of the total and differential inclusive  $B^+$  hadron cross sections in  $pp$  collisions at  $\sqrt{s} = 13$  TeV, Phys. Lett. B **771**, 435 (2017), arXiv:1609.00873.
- [44] R. Aaij et al. (LHCb), Prompt charm production in  $pp$  collisions at  $\sqrt{s} = 7$  TeV, Nucl. Phys. B **871**, 1 (2013), arXiv:1302.2864.
- [45] R. Aaij et al. (LHCb), Measurement of  $J/\Psi$  production in  $pp$  collisions at  $\sqrt{s} = 7$  TeV, Eur. Phys. J. C **71**, 1645 (2011), arXiv:1103.0423.
- [46] R. Aaij et al. (LHCb), Measurement of  $\Psi(2S)$  meson production in  $pp$  collisions at  $\sqrt{s} = 7$  TeV, Eur. Phys. J. C **72**, 2100 (2012), [Erratum: Eur.Phys.J.C 80, 49 (2020)], arXiv:1204.1258.
- [47] R. Aaij et al. (LHCb), Measurement of  $B$  meson production cross-sections in proton-proton collisions at  $\sqrt{s} = 7$  TeV, JHEP **08**, 117, arXiv:1306.3663.
- [48] R. Aaij et al. (LHCb), Forward production of  $\Upsilon$  mesons in  $pp$  collisions at  $\sqrt{s} = 7$  and 8 TeV, JHEP **11**, 103, arXiv:1509.02372.
- [49] R. Aaij et al. (LHCb), Measurement of the inclusive  $\phi$  cross-section in  $pp$  collisions at  $\sqrt{s} = 7$  TeV, Phys. Lett. B **703**, 267 (2011), arXiv:1107.3935.



- [50] R. Aaij et al. (LHCb), Measurement of  $\Psi(2S)$  production cross-sections in  $pp$  collisions at  $\sqrt{s} = 7$  and 13 TeV, *Eur. Phys. J. C* **80**, 185 (2020), arXiv:1908.03099.
- [51] R. Aaij et al. (LHCb), Production of  $J/\Psi$  and  $\Upsilon$  mesons in  $pp$  collisions at  $\sqrt{s} = 8$  TeV, *JHEP* **06**, 064, arXiv:1304.6977.
- [52] R. Aaij et al. (LHCb), Measurements of prompt charm production cross-sections in  $pp$  collisions at  $\sqrt{s} = 13$  TeV, *JHEP* **03**, 159, [Erratum: *JHEP* 09, 013 (2016), Erratum: *JHEP* 05, 074 (2017)], arXiv:1510.01707.
- [53] R. Aaij et al. (LHCb), Measurement of the  $\eta_c(1S)$  production cross-section in  $pp$  collisions at  $\sqrt{s} = 13$  TeV, *Eur. Phys. J. C* **80**, 191 (2020), arXiv:1911.03326.
- [54] R. Aaij et al. (LHCb), Measurement of forward  $J/\Psi$  production cross-sections in  $pp$  collisions at  $\sqrt{s} = 13$  TeV, *JHEP* **10**, 172, [Erratum: *JHEP* 05, 063 (2017)], arXiv:1509.00771.
- [55] R. Aaij et al. (LHCb), Measurement of  $\Upsilon$  production in  $pp$  collisions at  $\sqrt{s} = 13$  TeV, *JHEP* **07**, 134, [Erratum: *JHEP* 05, 076 (2019)], arXiv:1804.09214.
- [56] R. Aaij et al. (LHCb), Study of  $\chi_b$  meson production in  $pp$  collisions at  $\sqrt{s} = 7$  and 8 TeV and observation of the decay  $\chi_b(3P) \rightarrow \Upsilon(3S)\gamma$ , *Eur. Phys. J. C* **74**, 3092 (2014), arXiv:1407.7734.
- [57] A. Andronic et al., Heavy-flavour and quarkonium production in the LHC era: from  $pp$  to heavy-ion collisions, *Eur. Phys. J. C* **76**, 107 (2016), arXiv:1506.03981.
- [58] G. Bíró, G. G. Barnaföldi, T. S. Biró, and K. Shen, Mass hierarchy and energy scaling of the Tsallis – Pareto parameters in hadron productions at RHIC and LHC energies, *EPJ Web Conf.* **171**, 14008 (2018), arXiv:1710.09062.
- [59] T. Sjöstrand, S. Ask, J. R. Christiansen, R. Corke, N. Desai, P. Ilten, S. Mrenna, S. Prestel, C. O. Rasmussen, and P. Z. Skands, An introduction to PYTHIA 8.2, *Comput. Phys. Commun.* **191**, 159 (2015), arXiv:1410.3012.
- [60] H. Han, Y.-Q. Ma, C. Meng, H.-S. Shao, Y.-J. Zhang, and K.-T. Chao,  $\Upsilon(nS)$  and  $\chi_b(nP)$  production at hadron colliders in nonrelativistic QCD, *Phys. Rev. D* **94**, 014028 (2016), arXiv:1410.8537.
- [61] N. A. Abdulov and A. V. Lipatov, Bottomonium production and polarization in the NRQCD with  $k_T$ -factorization. III:  $\Upsilon(1S)$  and  $\chi_b(1P)$  mesons, *Eur. Phys. J. C* **81**, 1085 (2021), arXiv:2011.13401.
- [62] N. A. Abdulov and A. V. Lipatov, Bottomonia production and polarization in the NRQCD with  $k_T$ -factorization. II:  $\Upsilon(2S)$  and  $\chi_b(2P)$  mesons, *Eur. Phys. J. C* **80**, 486 (2020), arXiv:2003.06201.
- [63] N. A. Abdulov and A. V. Lipatov, Bottomonia production and polarization in the NRQCD with  $k_T$ -factorization. I:  $\Upsilon(3S)$  and  $\chi_b(3P)$  mesons, *Eur. Phys. J. C* **79**, 830 (2019), arXiv:1909.05141.
- [64] A. Esposito, E. G. Ferreira, A. Pilloni, A. D. Polosa, and C. A. Salgado, The nature of X(3872) from high-multiplicity  $pp$  collisions, *Eur. Phys. J. C* **81**, 669 (2021), arXiv:2006.15044.